Influence of human Ect2 depletion and overexpression on cleavage furrow formation and abscission

Ravindra B. Chalamalasetty, Stefan Hümmer, Erich A. Nigg and Herman H. W. Silljé*

Max Planck Institute for Biochemistry, Department of Cell Biology, Am Klopferspitz 18, 82152 Martinsried, Germany

*Author for correspondence (e-mail: sillje@biochem.mpg.de)

Accepted 3 May 2006
Journal of Cell Science 119, 3008-3019 Published by The Company of Biologists 2006
doi:10.1242/jcs.03032

Summary

The guanine nucleotide-exchange factor (GEF) Ect2 is essential for cytokinesis. Here we studied the subcellular localization of Ect2 and examined the consequences of either depleting or overexpressing Ect2 in human cells. We show that in mitotic cells Ect2 localizes to the central spindle and to the cell cortex. The latter association is mediated through a PH domain in Ect2 and central spindle localization requires the MKlp1-MgcRacGAP and MKlp2–Aurora-B complexes. Ect2 directly interacts with MKlp1-MgcRacGAP through its BRCT domain, whereas MKlp2–Aurora-B probably exerts a regulatory role in Ect2 central spindle targeting. Depletion of Ect2 impaired cleavage furrow formation and RhoA and Citron kinase failed to accumulate at the cleavage furrow. Ect2 displacement from the central spindle revealed that physiological levels of this protein in this location are not crucial for RhoA activation and cytokinesis. In cells overexpressing appropriate N-terminal Ect2 fragments, RhoA and Citron kinase localized to the cleavage furrow and ingression occurred, but abscission failed. This failure could be correlated with the persistence of these fragments at structures surrounding the midbody, suggesting that abscission requires the displacement of Ect2 from the contractile ring and its re-import into the nucleus.

Supplementary material available online at
http://jcs.biologists.org/cgi/content/full/119/14/3008/DC1

Key words: Cytokinesis, Ect2, Central spindle, Cleavage furrow, Abscission

Introduction

To maintain genomic stability from one cell generation to the next, dividing cells must faithfully segregate their chromosomes and subsequently carry out cytokinesis. In eukaryotic cells, these processes depend on a highly dynamic microtubule-based structure, the mitotic spindle. In animal cells, the spindle not only brings about the mechanical separation of chromosomes, but also determines the placement of the cleavage furrow. Although early studies, mostly performed in very large cells (notably fertilized eggs), have emphasized a crucial role of astral microtubules in cleavage-plane positioning (Devore et al., 1989), more recent data from embryos and cultured cells identify the central spindle as an important regulator of cytokinesis (Glotzer, 2001). This latter idea is supported by the finding that several proteins associated with the central spindle are required for proper cytokinesis. These include the mitotic kinesins MKlp1 (Kuriyama et al., 2002; Matuliene and Kuriyama, 2002) and MKlp2 (Hill et al., 2000; Neef et al., 2003). MKlp1 forms a stable complex, also known as centralspindlin (Mishima et al., 2002), with the GTPase-activating protein MgcRacGAP (Hirose et al., 2001), whereas MKlp2 associates with the mitotic kinases Aurora-B and Plk1 (Barr et al., 2004; Gruneberg et al., 2004; Neef et al., 2003). These complexes are required for the proper formation of the central spindle. Moreover, they may be involved in relaying information from the central spindle to the cortex, thereby determining the timing and positioning of actomyosin ring assembly. Following contractile ring assembly at the cortex, cleavage furrow ingression and subsequent abscission complete cytokinesis.

Another protein thought to play a key role in cytokinesis is Ect2 (Epithelial cell transforming protein 2), a guanine nucleotide exchange factor (GEF) for Rho family GTPases (Tatsumoto et al., 1999). The role of this protein in cytokinesis first emerged from studies in *Drosophila*, where the pebble gene (*pbl*) product (the ortholog of mammalian Ect2) was shown to be required for contractile ring formation and cytokinesis after cellularization of the syncytial embryo (Hime and Saint, 1992; Lehner, 1992; Prokopenko et al., 1999; Somers and Saint, 2003). Mammalian Ect2 is a member of the Dbl (diffuse B-cell lymphoma) family of GEFs and was originally identified as a transforming protein in an expression-cloning assay (Miki et al., 1993). In addition to a catalytic GEF domain, Ect2 comprises a PH (pleckstrin homology) domain and two BRCT repeats. Cytokinesis was impaired following either microinjection of anti-Ect2 antibodies or overexpression of an N-terminal fragment containing the BRCT domains (Tatsumoto et al., 1999). This N-terminal domain is able to interact with the C-terminal GEF domain (Saito et al., 2004), suggesting that the cytokinesis failure produced by its overexpression results from interference with the GEF activity of Ect2 (Kimura et al., 2000). Recently, siRNA studies have confirmed the essential role of Ect2 during cytokinesis (Kim et al., 2005; Yüce et al., 2005). Relevant to its molecular function,

Ect2 has been shown to increase the exchange activity of the small GTPases RhoA, Rac1 and Cdc42 in vitro (Tatsumoto et al., 1999). However, only RhoA is known to function in cytokinesis in vivo and recent findings suggest that RhoA is indeed the main downstream target of Ect2 (Kamijo et al., 2006; Kimura et al., 2000; Nishimura and Yonemura, 2006; Yüce et al., 2005). As RhoA functions in actomyosin ring formation and cleavage furrow ingression, the regulation of this GTPase is clearly crucial for cytokinesis (Glotzer, 2001).

In this study, we have explored the roles of human Ect2 in cell division as well as the mechanisms controlling its localization. Our results indicate that Ect2 localizes to both the central spindle and the cell cortex. We identify domains within Ect2 as well as interacting proteins that are required for localization to these specific subcellular structures. We also show that depletion of Ect2 results in cytokinesis failure through impairment of cleavage furrow formation. By contrast, overexpression of certain N-terminal, BRCT-domain-containing fragments of Ect2 interfere with abscission. Accordingly, we have investigated the possible cause(s) for this abscission defect.

Results

Localization of endogenous Ect2 in human cells

To study the function and localization of human Ect2, specific antibodies were raised against an N-terminal domain (residues 1-388) (supplementary material Fig. S1). The localization of endogenous Ect2 was then examined by indirect immunofluorescence microscopy. In interphase cells, Ect2 localized predominantly to the cell nucleus, but some cortical staining could also be observed, especially at cell-cell contacts (Fig. 1A). In mitotic cells, affinity-purified anti-Ect2 antibodies stained predominantly the central spindle and spindle poles during anaphase as well as the midbody and the reformed nuclei during telophase (Fig. 1A), in agreement with previous studies (Liu et al., 2004; Tatsumoto et al., 1999). In addition, we also observed staining of the cell cortex throughout mitosis (Fig. 1A). Upon depletion of Ect2 by siRNA, the staining of both spindle structures and the cell cortex was strongly reduced, attesting to its specificity (Fig. 1A). Efficient depletion of Ect2 was also confirmed by western blot analysis (Fig. 1B).

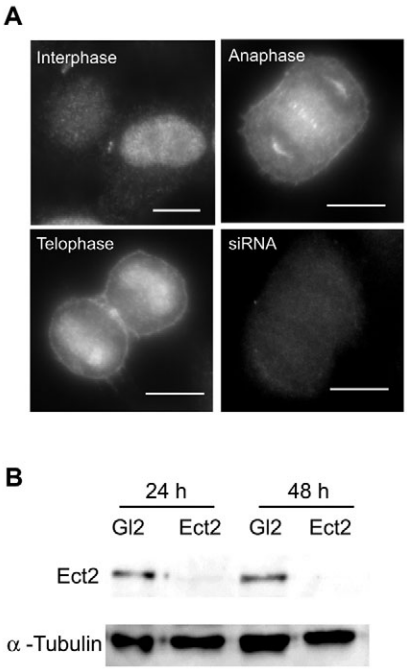

Fig. 1. Ect2 localizes to the central spindle and the cortex of mitotic cells. (A) HeLa S3 cells grown on coverslips were fixed with paraformaldehyde and permeabilized with Triton X-100. Cells were then stained with anti-Ect2 antibodies. Different cell-cycle phases and a control cell treated for 24 hours with a siRNA targeting Ect2 are shown. Bar, 10 μm. (B) HeLa S3 cells were treated with GL2 and Ect2 siRNAs for 24 and 48 hours. Subsequently, cell lysates were prepared and proteins were separated by SDS-PAGE and transferred onto nitrocellulose membranes. These were probed with anti-Ect2 antibodies (upper panel) and, as a loading control, with anti-α-tubulin antibodies (lower panel).

Identification of Ect2 domains involved in subcellular targeting

To determine which domains within Ect2 are required for targeting the protein to the central spindle and cell cortex, respectively, different myc-tagged Ect2 fragments (Fig. 2A) were transiently expressed in HeLa S3 cells. A C-terminal fragment of Ect2 (residues 320-883) showed prominent association with the cell cortex, but did not localize to the central spindle (Fig. 2A,B). Further truncation analysis revealed that the PH domain was required for targeting Ect2 to the cell cortex (Fig. 2A,B). Considering that PH domains constitute lipid-binding motifs (Blomberg et al., 1999), this suggests that the cortex association of Ect2 involves a direct interaction with the plasma membrane. N-terminal fragments of Ect2 localized to the central spindle but were absent from the cell cortex (Fig. 2A,C), confirming and extending previous results (Tatsumoto et al., 1999). In particular, fragments containing a full BRCT domain ($Ect2_{1-420}$ and $Ect2_{1-333}$) localized to the central spindle, whereas a truncated BRCT domain ($Ect2_{1-288}$) was absent from the central spindle (Fig. 2A,C). Thus, a full BRCT domain including both BRCT repeats was found to be essential for central spindle localization.

Influence of MKlp1-MgcRacGAP and MKlp2–Aurora-B complexes on Ect2 localization

To determine which proteins are required for Ect2 localization to the central spindle, we depleted MKlp1, MKlp2, Aurora-B and MgcRacGAP from HeLa S3 cells, using previously validated siRNA duplex oligonucleotides. In agreement with previous reports (Hirose et al., 2001; Matuliene and Kuriyama, 2002; Neef et al., 2003; Terada et al., 1998), inhibiting the functions of all four proteins resulted in a significant increase in multinucleated cells, indicative of cytokinesis defects (data not shown). In some cells (presumably those showing partial depletion) structures resembling central spindles were still detectable, although they were often strongly deformed, consistent with the view that all the above proteins contribute to central spindle formation (Fig. 3A). Importantly, depletion of all four proteins abolished the association of Ect2 with residual central spindle and midbody structures, although Ect2 levels were not affected (Fig. 3A and data not shown). Normal

Ect2 localization was observed in a control GL2 siRNA (Fig. 3A). We conclude that MKlp1, MKlp2, Aurora-B and MgcRacGAP were all required for proper localization of Ect2 to the central spindle.

The above results suggested that Ect2 might directly interact with one or more of the above central spindle proteins. To explore this possibility, co-immunoprecipitation experiments were performed on HeLa S3 cells that had been synchronised by an aphidicolin and nocodazole block-release protocol and harvested when most cells were present in anaphase or telophase. Endogenous Ect2 was immunoprecipitated using anti-Ect2 antibodies and immune complexes were probed by western blotting for the presence of the different central spindle components. As a control, immunoprecipitates prepared with pre-immune antibodies were analyzed in parallel. Whereas none of the proteins were observed in control immunoprecipitates, MKlp1 and MgcRacGAP could readily be detected in Ect2 immunoprecipitates, but Aurora-B and MKlp2 were absent (Fig. 3B). The interaction of Ect2 with the MKlp1-MgcRacGAP complex was further confirmed by co-immunoprecipitation experiments using anti-MKlp1 (Fig. 3C) and anti-MgcRacGAP antibodies (Fig. 3D), respectively. These data suggest that MKlp1-MgcRacGAP is directly required for targeting Ect2 to the central spindle, whereas MKlp2–Aurora-B is more likely to perform an indirect, regulatory role.

A physiological level of Ect2 is not required at the central spindle for cytokinesis

We next asked whether the N-terminal fragments that localize to the central spindle would be able to displace endogenous Ect2 from this site. To specifically detect endogenous Ect2 in these experiments, we used an antibody directed against C-terminal epitopes within the protein. This antibody recognized endogenous Ect2 on western blots containing whole-cell lysates (Fig. S2). Examination of transiently transfected cells showed that overexpression of two distinct BRCT-domain-containing fragments (spanning residues 1-420 and 1-333, respectively) caused the displacement of endogenous Ect2 from the central spindle (Fig. 4A). By contrast, a smaller fragment ($Ect2_{1-288}$), which contained a truncated BRCT domain and hence did not localize to the central spindle, was unable to displace endogenous Ect2 from this location (Fig. 4A). This suggests that overexpressed Ect2 fragments could compete with endogenous Ect2 for binding sites on the MKlp1-MgcRacGAP complex only if they contained the complete BRCT domain. In support of this interpretation, the two BRCT-domain-containing Ect2 fragments, but not the shorter Ect2 fragment, could be shown to interact with MKlp1-MgcRacGAP in co-immunoprecipitation assays (Fig. 4B).

Most cells (>50%; see also Fig. 7A) expressing $Ect2_{1-333}$ became bi- and multi-nucleated after 48 hours of expression, indicative of a cytokinesis failure induced by this fragment. By contrast, although the larger N-terminal $Ect2_{1-420}$ also

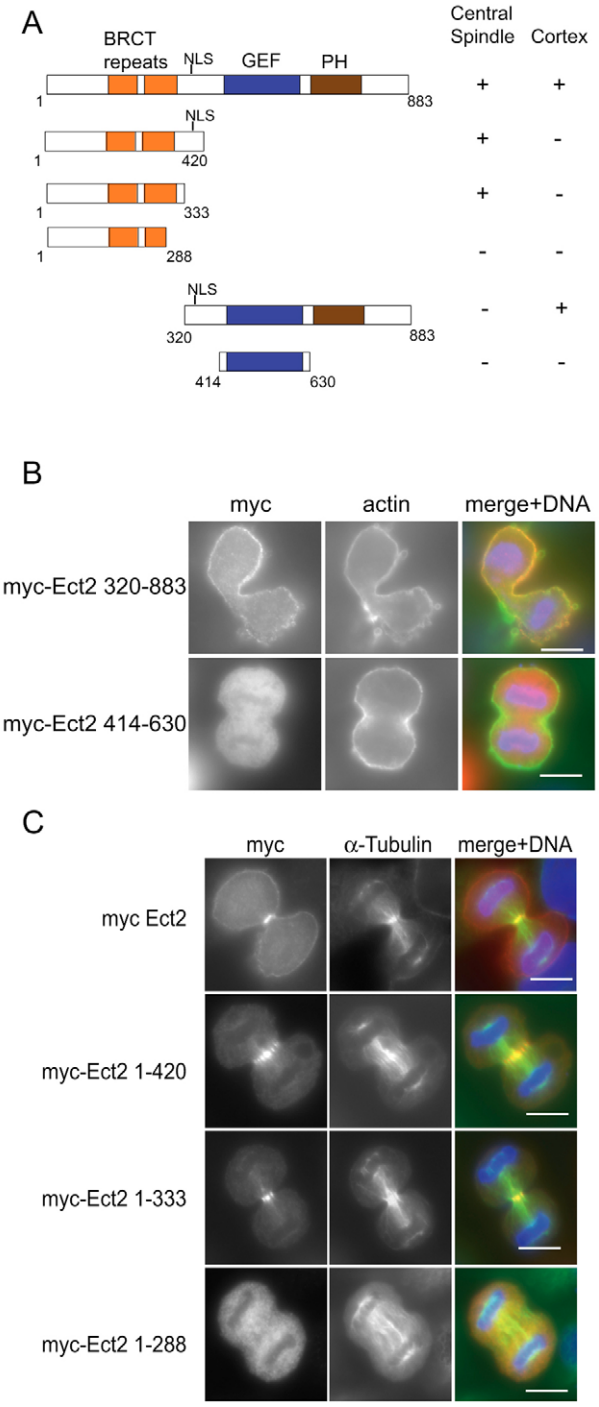

Fig. 2. The BRCT domain targets Ect2 to the central spindle, whereas the PH domain is required for cell cortex localization. (A) Schematic representation of different Ect2 domains and the ability of various N- and C-terminal fragments to localize to the central spindle and the cell cortex. + indicates presence and – absence of localization to the central spindle and cortex. (B) HeLa S3 cells were grown on coverslips and transiently transfected for 36 hours with the indicated myc-Ect2 fragments before fixation with paraformaldehyde and permeabilization with Triton X-100. Cells were stained with anti-myc 9E10 antibodies (left) and FITC-phalloidin (middle). Merged images are shown on the right with 9E10 in red, actin in green and DNA stained with DAPI in blue. (C) HeLa S3 cells were transfected for 36 hours with the indicated myc-Ect2 constructs, fixed and permeabilized as described in B and stained with anti-myc 9E10 antibodies (left) and anti α-tubulin antibodies (middle). Merged images are shown on the right, with 9E10 in red, α-tubulin in green and DNA stained with DAPI in blue. Bars, 10 μm.

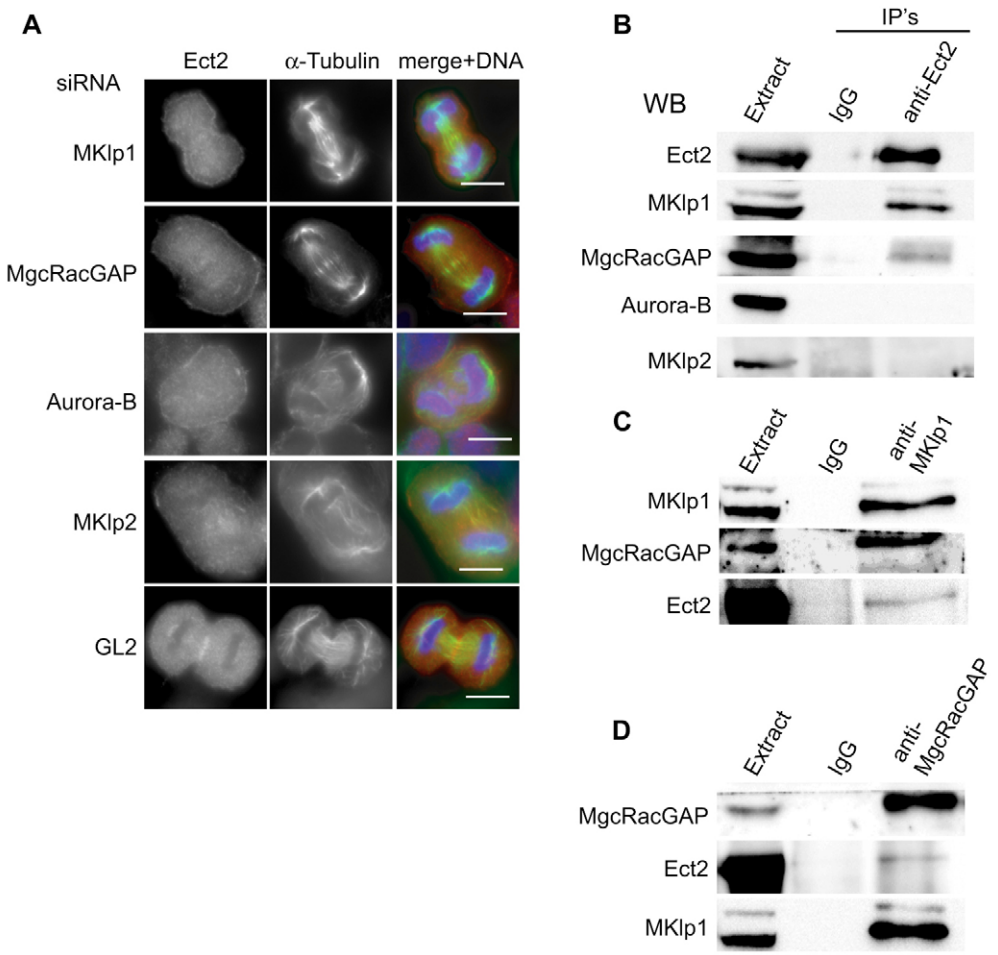

Fig. 3. The MKlp1-MgcRacGAP and MKlp1–Aurora-B complexes are both required for localizing Ect2 to the central spindle. (A) HeLa S3 cells were treated with control (GL2), MKlp1, MgcRacGAP, Aurora-B and MKlp2 siRNAs for 36 hours before fixation and permeabilization with paraformaldehyde and Triton X-100, respectively. Subsequently, cells were stained with anti-Ect2 (left) and anti-α-tubulin (middle) antibodies. Merged images are shown on the right with Ect2 in red, α-tubulin in green and DNA stained with DAPI in blue. Bars, 10 μm. In all cells, the focal plane was adjusted to visualize central spindle rather than cortex staining. (B) Cell lysates from anaphase/telophase synchronized HeLa S3 cells were used for immunoprecipitations (IP's) with anti-Ect2 antibodies (anti-Ect2) or pre-immune antibodies (IgG). Immunoprecipitates and input lysates (Extract) were then probed by western blotting with antibodies against the indicated proteins. (C) Immunoprecipitation using anti-MKlp1 antibodies. (D) Immunoprecipitation using anti-MgcRacGAP antibodies.

displaced endogenous Ect2 from the central spindle, this protein did not cause major cytokinesis defects (7%; see also Fig. 7A). This surprising finding indicates that physiological levels of Ect2 do not need to localize to the central spindle for cytokinesis to occur. Moreover, because both BRCT-domain-containing fragments displaced endogenous Ect2 equally well (Fig. 4A), it follows that the cytokinesis defect caused by only one of the two fragments ($Ect2_{1\text{-}333}$) does not result from Ect2 displacement. The mode of action of this dominant-negative Ect2 construct is addressed below.

Interference with cleavage furrow formation and abscission by manipulation of Ect2 levels

To study the molecular mechanism(s) underlying the cytokinesis defect produced by overexpression of the BRCT-containing fragment ($Ect2_{1\text{-}333}$), a tetracycline-inducible cell line stably expressing this myc-tagged fragment was generated (Fig. 5A). Mitotic progression in cells expressing this domain (Fig. 5B, upper panel) was then compared with control cells (Fig. 5B, lower panel) and cells that had been depleted of Ect2 by siRNA (Fig. 5B, middle panel). In cells overexpressing the BRCT-containing fragment ($Ect2_{1\text{-}333}$), central spindle formation, cleavage furrow ingression and midbody formation all appeared to be normal (Fig. 5B, upper panel). Subsequently, however, abscission failed and cells became binucleate. In comparison, bipolar spindle formation and initial central spindle formation also looked normal in Ect2-depleted cells, indicating that Ect2, unlike MKlp1, MKlp2, MgcRacGAP and Aurora-B, was not required for central spindle formation per se (Fig. 5B, middle panel). However, in Ect2-depleted cells at late anaphase, spindles were clearly abnormal. Specifically, they became increasingly voluminous and microtubules extended all over the equatorial cortical region. At later stages, midbody formation was absent and, instead, a central-spindle-like structure continued to persist between two reforming nuclei. Finally, interphase microtubule networks formed in

binucleate cells that had failed to undergo cytokinesis. The most plausible explanation for the phenotype of Ect2-depleted cells is that the cleavage furrow failed to ingress.

To confirm the strikingly distinct phenotypes produced by overexpression of a BRCT-containing fragment of Ect2 and siRNA-mediated depletion of Ect2, respectively, live-cell imaging was performed (see Movies in supplementary material). As summarized by the stills shown in Fig. 5C, cleavage furrows formed and ingressed in most cells expressing the BRCT-containing fragment of Ect2 (38 out of 48 cells analyzed; four cells proceeded normally and six died; Fig. 5C, top panel). The process was largely indistinguishable from that in control cells treated with GL2 oligonucleotides (Fig. 5C, lower panel), except that the metaphase to anaphase transition was accompanied by extensive membrane blebbing in more than 50% of the cells expressing Ect2 fragment (Fig. 5C, top panel). The cause of this blebbing is not entirely clear, but because bleb formation requires dissociation of the cytoskeleton from the plasma membrane (Charras et al., 2005), it probably indicates the occurrence of abnormal cytoskeletal rearrangements during this phase of mitosis. We also noticed that, on average, these cells spent a longer time in mitosis than controls, with large cell-to-cell variability (249±69 minutes). Moreover, these cells sometimes seemed to have difficulties in positioning the cleavage furrow properly. Often it was also seen that during apparent division one cell had already flattened on the culture dish, whereas the other remained rounded, suggesting that the cytoplasmic contents of these dividing cells had practically been separated. Ultimately, however, these cells failed abscission and instead fused back to form single binucleate cells.

In striking contrast to the above phenotype, most of the Ect2-depleted cells showed no clear cleavage furrow formation or ingression; instead, most cells (23 out of 42 cells analyzed) exited mitosis without showing any signs of having attempted cytokinesis (Fig. 5C, upper middle panel). Only 14 cells showed partial ingression and five cells showed normal division. Ect2-depleted cells spent 87±24 minutes in mitosis, which is similar to control cells (Fig. 5C, lower panel). When using siRNAs that depleted Ect2 less efficiently (data not shown), an increasing number of these Ect2-depleted cells could be seen to form furrows which then began to ingress, before they regressed again (Fig. 5C, lower middle panel). We conclude that complete Ect2 depletion prevents cleavage furrow formation, whereas partial depletion allows the formation of furrows, which then, however, fail to complete ingression.

Effect of Ect2 levels on targeting of RhoA and Citron kinase

One of the early crucial steps in cytokinesis is the activation of RhoA (Bement et al., 2005). This GTPase then controls several proteins that regulate the dynamics of the actin cytoskeleton, leading to contractile ring formation and contraction (Glotzer, 2001). A recent study in *Drosophila* showed that both Rho1

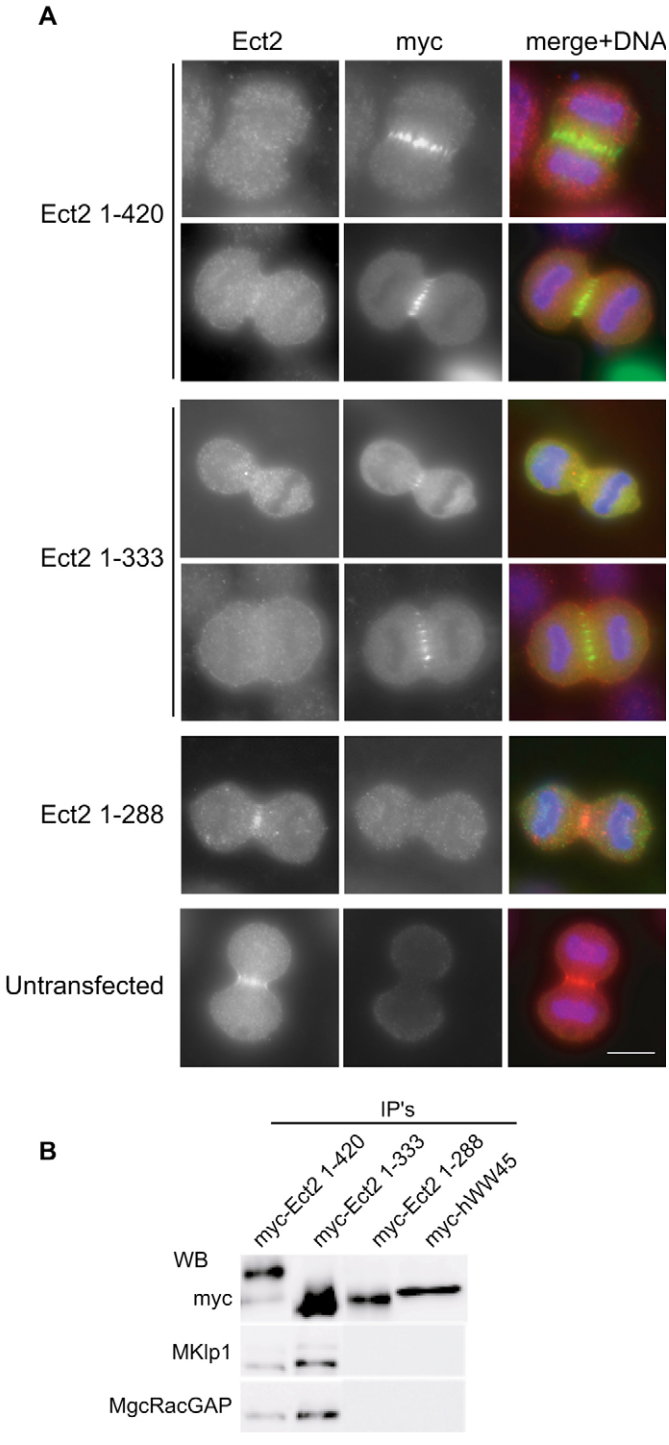

Fig. 4. Ect2 displacement from the central spindle does not interfere with cytokinesis. (A) HeLa S3 cells were grown on coverslips and transiently transfected for 36 hours with the indicated myc-Ect2 constructs before fixation and permeabilization with formaldehyde and Triton X-100. Cells were then stained with anti-myc 9E10 antibodies (middle) and antibodies recognizing a C-terminally located epitope on endogenous Ect2 (left). Merged images show transfected myc-Ect2 (9E10) in green, endogenous Ect2 in red and DNA stained with DAPI in blue. A control, non-transfected, cell is shown in the bottom row. Note that this antibody required a simultaneous fixation-permeabilization protocol, so that cortex localization of Ect2 was difficult to see. Bar, 10 μm. (B) Transiently overexpressed myc-Ect2 fragments were immunoprecipitated from HeLa S3 cells synchronized at anaphase/telophase, using the anti-myc 9E10 antibody (IP's). For control, an unrelated myc-tagged hWW45 construct was transfected and analyzed in parallel. Samples were then probed by western blotting with antibodies against the indicated proteins.

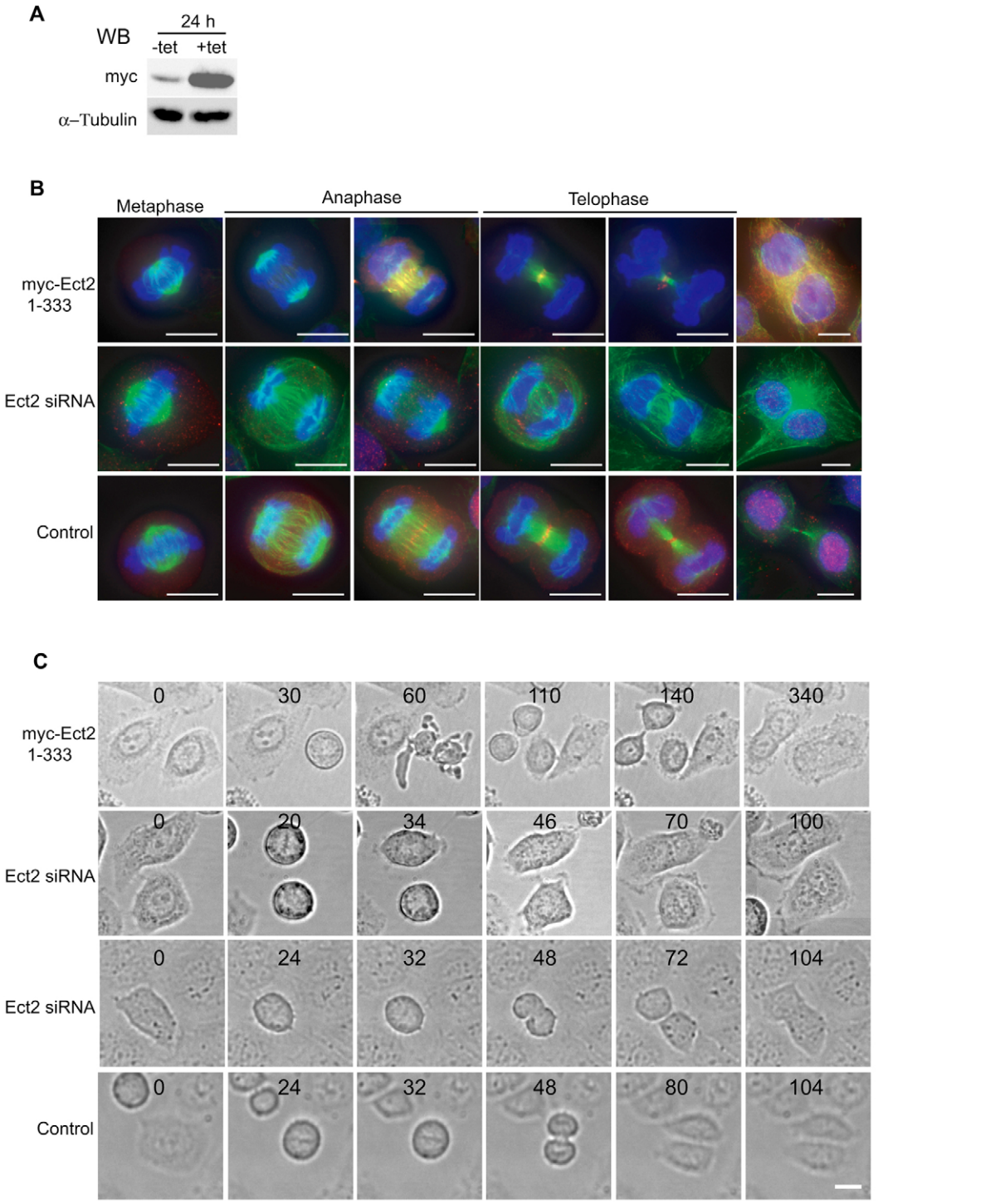

Fig. 5. In Ect2-depleted cells cleavage furrow formation is impaired, whereas in cells overexpressing the $Ect2_{1\text{-}333}$ fragment cell abscission fails. (A) Western blots with lysates from a stable tetracycline-inducible myc-$Ect2_{1\text{-}333}$ cell line, with or without induction with tetracycline for 24 hours. Blots were probed with anti-myc 9E10 antibodies to illustrate induction of the Ect2 fragment and with anti-α-tubulin antibodies to show equal loading. (B) HeLa S3 cells were treated for 24 hours with either GL2 (control) or Ect2 siRNAs and, in parallel, the inducible myc-$Ect2_{1\text{-}333}$ cell line was treated for 24 hours with tetracycline. After fixation and permeabilization with paraformaldehyde and Triton X-100, respectively, the myc-$Ect2_{1\text{-}333}$ expressing cells were stained with anti-myc 9E10 antibodies (red), anti α-tubulin antibodies (green) and DAPI (blue) and the siRNA-treated cells were stained with anti-Ect2 antibodies (red), anti-α-tubulin antibodies (green) and DAPI (blue). Images represent merged deconvolved series of *Z* stacks through each cell. (C) Live-cell imaging of tetracycline (tet)-induced myc-$Ect2_{1\text{-}333}$ HeLa S3 cells (upper panel), Ect2-depleted HeLa S3 cells (middle two panels) and HeLa S3 cells treated with GL2 control oligonucleotides (lower panel). Images were taken every 2 minutes and only representative frames are shown. In cells expressing myc-$Ect2_{1\text{-}333}$, time '0' was attributed to the last frame in which the cell on the right side still showed an interphase appearance. Similarly, in Ect2-depleted and GL2-treated control cells, time '0' was attributed to the last frame in which the relevant cells still showed an interphase appearance. Bars, 10 μm.

(RhoA) and one of its downstream targets, Sticky (Citron kinase), required *pbl* (Ect2) for proper localization to the contractile ring (Shandala et al., 2004). In *Drosophila*, both Rho1 and Sticky are required for cytokinesis, but in mammalian cells the role of Citron kinase in cytokinesis remains controversial (Di Cunto et al., 2000). Depletion of Citron kinase in HeLa S3 cells resulted, however, in a strong binucleate phenotype indicating that Citron kinase is essential for cytokinesis in HeLa S3 cells (Fig. S3) (see also Grüneberg et al., 2006; Kamijo et al., 2006).

We next analyzed the localization of RhoA and Citron kinase during cytokinesis in human cells. In undisturbed cells, both proteins localized to the contractile ring during cytokinesis (Fig. 6A,B, top rows), confirming previous results (Eda et al., 2001; Mabuchi et al., 1993; Madaule et al., 1998). The localization was more difficult to analyze in Ect2-depleted cells, as most of these cells do not form any detectable cleavage furrows. However, in those few Ect2-depleted cells that did show some cleavage furrow formation both RhoA and Citron kinase were strongly diminished at this site (Fig. 6A,B, middle row), confirming and extending recent observations (Yüce et al., 2005; Kamijo et al., 2006). These data show that Ect2 regulates RhoA, as well as its downstream target Citron kinase, also in human cells.

In contrast to the situation in Ect2-depleted cells, RhoA and Citron kinase could readily be detected at the cleavage furrow in cells expressing the N-terminal BRCT-containing Ect2 fragment (Fig. 6A,B, bottom row). This result is in line with the observation that these cells showed cleavage furrow formation and ingression (Fig. 5). Taken together, our data indicate that the inability to target RhoA and Citron kinase to the cleavage furrow may constitute the main reason for the cytokinesis defects observed in Ect2-depleted cells. On the other hand, because RhoA and Citron kinase were properly targeted to the cleavage furrow in cells expressing the N-terminal Ect2 fragment, it follows that cytokinesis failure in these latter cells must result through another mechanism.

N-terminal Ect2$_{1-333}$ causes abscission failure

To investigate why the N-terminal Ect2$_{1-333}$ fragment, but not the Ect2$_{1-420}$ fragment, caused cytokinesis defects, three additional N-terminal Ect2 mutant constructs, Ect2$_{1-360}$, Ect2$_{1-370}$ and Ect2$_{1-388}$ were studied. Overexpression of Ect2$_{1-360}$ and Ect2$_{1-370}$ also resulted in the formation of binucleate cells, but the larger Ect2$_{1-388}$ fragment did not interfere with cytokinesis (Fig. 7A). These effects could not be attributed to differences in expression levels as determined by western blot analysis (Fig. 7B). Interestingly, all those fragments that caused cytokinesis failure localized predominantly to the cytoplasm, whereas those fragments that did not interfere with cytokinesis localized to the nucleus. This is in agreement with the presence of a putative NLS in the larger fragments (between residues 348 and 373) (Fig. 2A). We reasoned, therefore, that the abscission failure produced by certain mutant Ect2 proteins could result from an inability of these mutants to be back-imported in the reforming telophase nucleus. To test this idea, three SV40 nuclear localization signals were added to the N-terminus of the smallest Ect2 fragment (Ect2$_{1-333}$). This fragment still associated with the central spindle in mitotic cells (data not shown), but now localized to the nucleus in interphase cells (Fig. 7C).

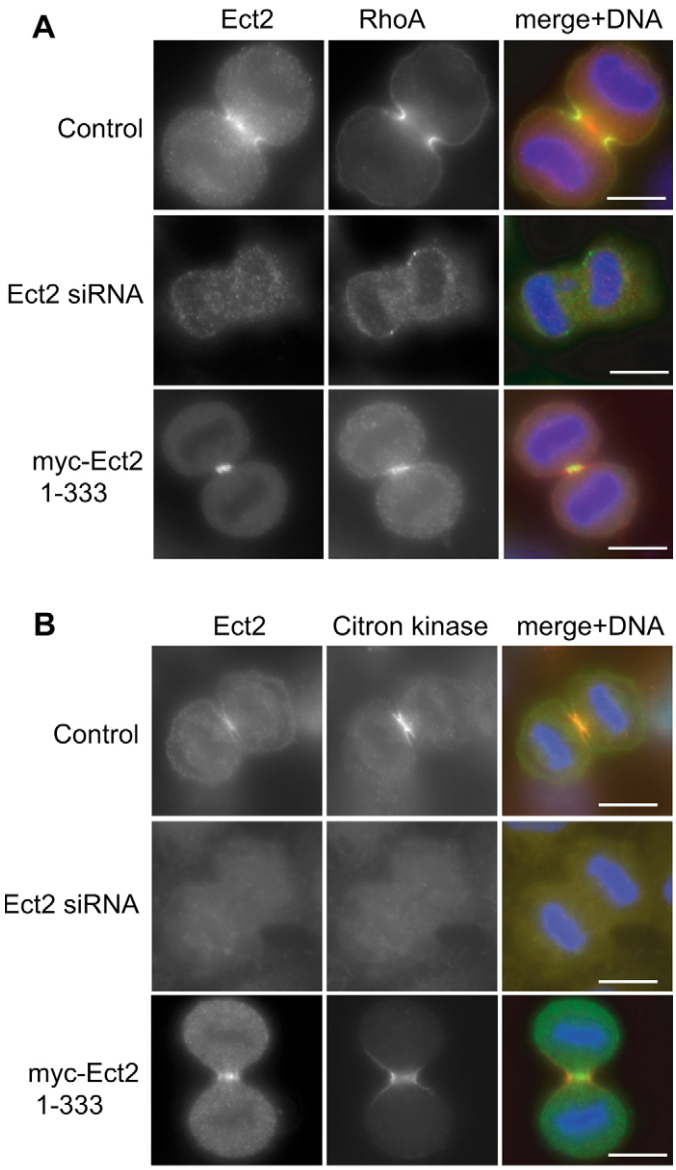

Fig. 6. Ect2 targets RhoA and Citron kinase to the cleavage furrow. (A) HeLa S3 cells were treated for 36 hours with control (GL2) or Ect2 siRNAs and the myc-Ect2$_{1-333}$-expressing cell line was induced for 36 hours with tetracycline. After fixation and permeabilization with 10% TCA and Triton X-100, siRNA-treated cells (upper and middle panels) were stained with anti-Ect2 (left, red) and anti-RhoA (middle, green) antibodies. The stable cell line (lower panel) was stained with anti-myc 9E10 (left, green) and anti-RhoA (middle, red) antibodies. Merged images are shown on the right with DNA in blue. (B) Cells were fixed with paraformaldehyde containing Triton X-100 and stained with anti-Citron kinase antibodies. Merged pictures are shown on the right with Ect2 and myc, respectively, in green, Citron kinase in red and DNA in blue. Bars, 10 μm.

Importantly, this fragment was much less potent in inducing cytokinesis defects than the corresponding fragment lacking the NLS (Fig. 7A), indicating that nuclear back-import can partially prevent the abscission defects induced by N-terminal Ect2 fragments. In a converse experiment, we also mutated the putative NLS sequences in the Ect2$_{1-388}$ fragment and asked whether interference with nuclear back-import would enhance

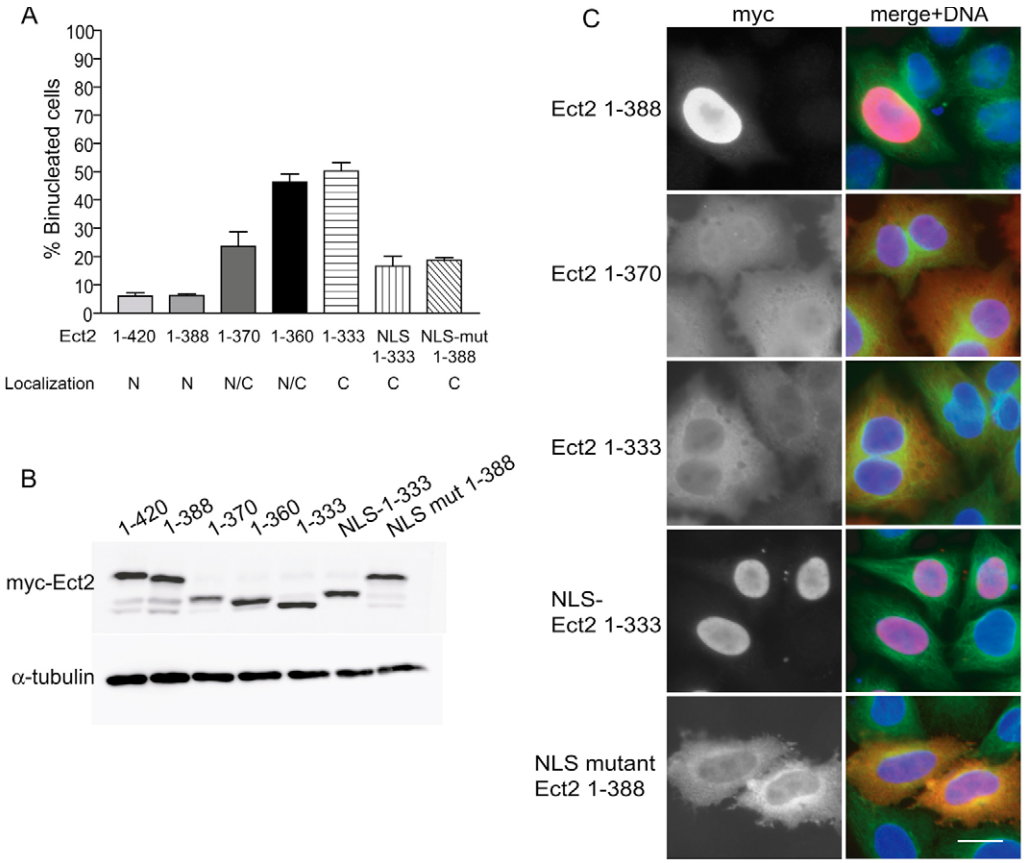

Fig. 7. Influence of nuclear localization on ability of Ect2 N-terminal fragments to interfere with cytokinesis. (A) The myc-tagged Ect2 constructs, $Ect2_{1-420}$, $Ect2_{1-388}$, $Ect2_{1-370}$, $Ect2_{1-360}$, $Ect2_{1-333}$, $Ect2_{1-333}$ containing three SV40 NLS motifs (NLS 1-333) and $Ect2_{1-388}$ with a mutated NLS (NLS mut 1-388) were transfected for 48 hours into HeLa S3 cells before fixation with paraformaldehyde and permeabilization with Triton X-100. Cells were then stained with anti-myc 9E10 antibodies and DAPI and analyzed for the presence of either a single nucleus or binucleation (and occasionally multi-nucleation). Histogram shows the results of three independent experiments (300 cells each) and bars indicate s.d. The localizations of the various constructs in interphase cells are indicated as N (nuclear), N/C (nuclear and cytoplasmic) and C (cytoplasmic). (B) Equal amounts of cell lysates, prepared from mitotic cells transfected with the constructs described in A, were separated by SDS-PAGE and probed by western blotting with anti-myc 9E10 antibody. Anti-α-tubulin detection is shown as a loading control. (C) HeLa S3 cells were transfected for 36 hours with the indicated myc-Ect2 constructs. Cells were then fixed with paraformaldehyde and permeabilized with Triton X-100, before they were stained with anti-myc 9E10 antibodies (red, left), anti-α-tubulin antibodies (green). Merged images including DNA stained with DAPI (blue) are shown on the right. Bar, 10 μm.

the ability of this fragment to produce abscission failure. However, although mutated $Ect2_{1-388}$ did localize to the cytoplasm, its overexpression only marginally increased the formation of binucleate cells when compared with its nuclear counterpart (19% versus 6%, respectively). Thus, although the NLS motifs contribute to determine the extent of cytokinesis failure produced by various Ect2 fragments, additional sequences flanking the central Ect2 NLS region must also be important.

In *Drosophila*, a double ring-like structure has been described during cell division, with Pebble present at the cortex and RacGAP50c (*Drosophila* ortholog of MgcRacGAP) at cortical microtubules, and the interaction between these proteins is thought to be crucial for Pebble activation (D'Avino et al., 2005; Somers and Saint, 2003; Yüce et al., 2005). Moreover, a unique midbody-associated ring structure important for abscission has recently been identified in human cells (Gromley et al., 2005). In light of these data, it is intriguing that the various Ect2 N-terminal fragments showed strikingly distinct localization patterns at the midbody. Whereas the $Ect2_{1-420}$ fragment showed a narrow localization at the midbody, the $Ect2_{1-333}$ fragment showed a distinctly peripheral localization extending to the cortex of the postmitotic bridge (Fig. 8A; see also Fig. 6A,B). Closer examination revealed that these structures often had a ring-like appearance (Fig. 8B). Moreover, both MKlp1 and MgcRacGAP, but not endogenous Ect2, were recruited to this structure (Fig. 8C and data not shown). Most importantly, this striking midbody-associated ring-like localization was only observed with Ect2 fragments that were able to interfere with abscission but not with any fragment that did not affect cytokinesis, including the $Ect2_{1-388}$ fragment that lacked the NLS (Fig. 8A,D). Thus, the abscission defect produced by overexpression of particular N-terminal Ect2 fragments clearly correlates with the sustained localization of these fragments in a ring-like structure at the cortex.

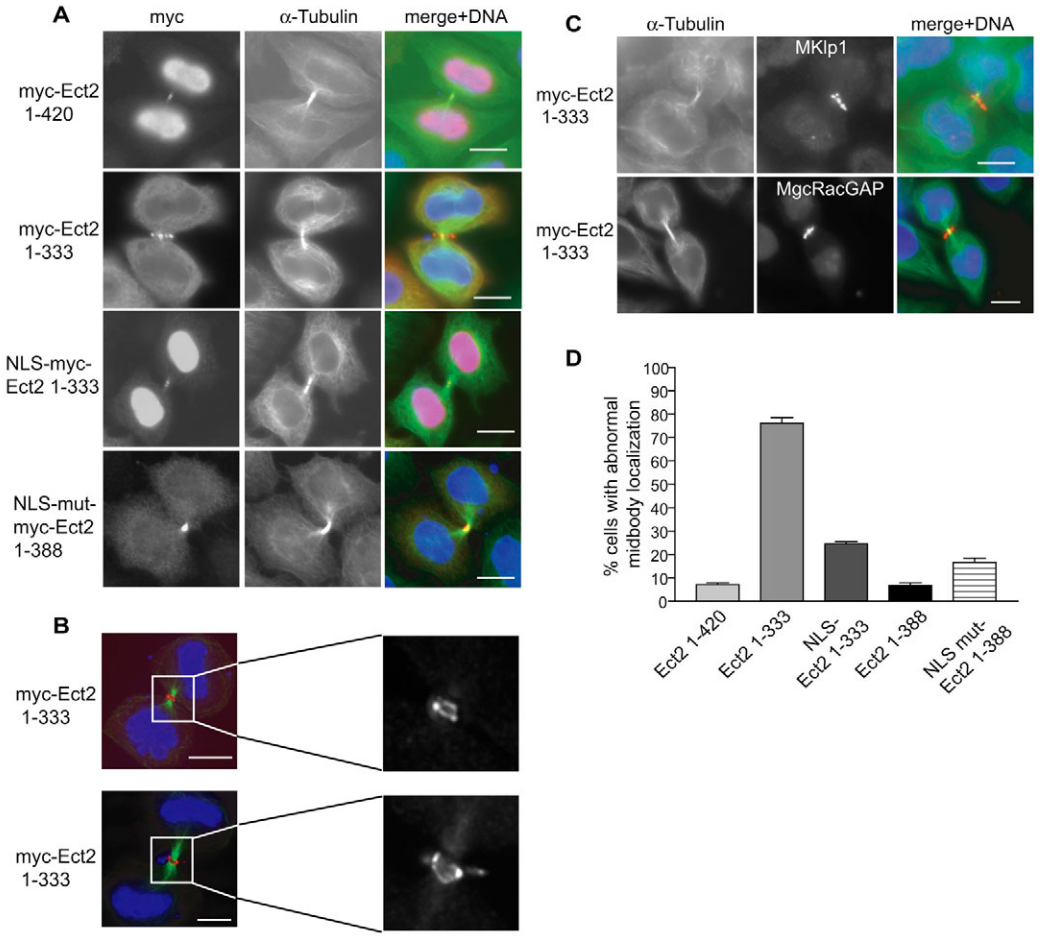

Fig. 8. Myc-Ect2$_{1\text{-}333}$ mislocalizes to a ring-like structure at the cell cortex near the midbody. (A) The indicated myc-Ect2 constructs were overexpressed for 48 hours in HeLa S3 cells before fixation with paraformaldehyde and permeabilization with Triton X-100. Cells were then stained with anti-myc 9E10 in red (left) and anti-α-tubulin antibodies in green (middle). Merged images including DNA stained with DAPI (blue) are shown on the right. (B) Higher resolution, deconvolved images of the Ect2$_{1\text{-}333}$ expressing cells. The three times enlargements on the right show only the myc-Ect2 staining. (C) The myc-Ect2$_{1\text{-}333}$ stable cell line was induced for 36 hours and stained with anti-MKlp1 and anti-MgcRacGAP antibodies (middle) in red, anti-α-tubulin antibodies (left) in green and DNA was labeled with DAPI in blue. Merged images are shown on the right. (D) Quantitative analysis of the number of cells showing displaced myc-Ect2 fragments around the midbody (as shown in A and B). Histogram shows the results of three independent experiments (120 cells each) and bars indicate s.d. Bars, 10 μm.

Discussion

Cytokinesis failure is increasingly recognized as an important source of genomic instability (Meraldi et al., 2002; Fujiwara et al., 2005; Margolis, 2005; Storchova and Pellman, 2004; Shi and King, 2005), but the molecular mechanisms underlying the regulation and execution of cytokinesis are only beginning to emerge (Glotzer, 2005). In this study, we have investigated the role of the human GEF Ect2 in cytokinesis. In a first series of experiments, we examined the parameters that determine the subcellular localization of Ect2 during mitosis. We found that Ect2 localizes to the central spindle through a process that requires its BRCT domain as well as the MKlp2–Aurora-B complex and the MKlp1-MgcRacGAP complex. In addition, we could show that Ect2 localizes to the cortex through a mechanism that depends on its C-terminal PH domain. Subsequently, we explored the consequences of either depleting Ect2 or overexpressing Ect2 fragments. Extensive depletion of Ect2 prevented cleavage furrow formation, whereas partial depletion allowed initial furrow ingression, followed by regression. In both cases, RhoA and Citron kinase failed to accumulate at the cell cortex and binucleate cells were ultimately formed.

The overexpression of various Ect2 constructs produced widely different phenotypes, yielding two results of particular interest. First, the expression of N-terminal Ect2$_{1\text{-}420}$ comprising an intact BRCT domain caused the displacement of endogenous Ect2 from the central spindle, but did not result in significant cytokinesis failure. This indicates that physiological levels of Ect2 GEF activity need not necessarily localize to the central spindle for successful cytokinesis. Second, the expression of the slightly shorter N-terminal Ect2$_{1\text{-}333}$ caused extensive cytokinesis failure, in agreement with a previous report (Saito et al., 2003). In these cells, RhoA and Citron kinase localized correctly to the cleavage furrow and furrow ingression occurred, but cells subsequently failed to undergo abscission. An investigation into the possible causes underlying this abscission showed that these fragments persisted on ring-like cortical structures surrounding the midbody. Based on the data obtained

with these fragments, we propose that, for successful abscission to occur, Ect2 apparently needs to be displaced from cortical midbody structures and be re-imported into the reforming telophase nucleus.

Ect2 localization to the central spindle

We could show that both the MKlp2–Aurora-B and the MKlp1-MgcRacGAP complex are required for proper targeting of Ect2 to the central spindle, but only the latter complex directly interacts with Ect2. Moreover, only the MKlp1-MgcRacGAP complex co-localized with Ect2 at the midbody in telophase cells (our unpublished data). This result falls in line with recent data showing that Ect2 binds directly to MgcRacGAP and that, during early mitosis, this interaction is negatively regulated by Cdk1, which phosphorylates Ect2 on T342 (Yüce et al., 2005). Our data have also revealed that the BRCT domain of Ect2 is required for binding to the MKlp1-MgcRacGAP complex. Since BRCT domains constitute phosphopeptide-binding domains (Clapperton et al., 2004; Williams et al., 2004), and because Aurora-B has been reported to phosphorylate MgcRacGAP and MKlp1 (Guse et al., 2005; Minoshima et al., 2003; Neef et al., 2006), it is tempting to speculate that Aurora-B might create a docking site for Ect2 binding on the MKlp1-MgcRacGAP complex. This would fit our data indicating that the MKlp2–Aurora-B complex plays a regulatory role in determining the central spindle association of Ect2.

Ect2 is required for RhoA and Citron kinase localization to the cleavage furrow

Recent data indicate that RhoA localizes to the cleavage furrow in its active (GTP bound) state, implying that Ect2 targets RhoA to the cleavage furrow by exchanging GDP for GTP (Bement et al., 2005; Yüce et al., 2005). In agreement with this conclusion, we have shown that Ect2 is essential for RhoA targeting to the cleavage furrow. Upon siRNA-mediated depletion of Ect2, RhoA was not localized to the cortex and no cleavage furrow formation occurred. Citron kinase, a downstream target of RhoA (Eda et al., 2001), also failed to localize to the contractile ring in Ect2-depleted cells. Although the role of RhoA in cytokinesis is well established, the function of Citron kinase was less clear. On the one hand, *Drosophila* Citron kinase is reported to be required for cytokinesis (D'Avino et al., 2004; Echard et al., 2004; Naim et al., 2004; Shandala et al., 2004) and HeLa cells transiently transfected with catalytically inactive Citron kinase failed cytokinesis (Madaule et al., 1998). On the other hand, Citron kinase$^{-/-}$ mice showed cytokinesis defects only in specialized cell types (Di Cunto et al., 2000). Our present siRNA depletion experiments clearly show that Citron kinase is essential for cytokinesis in cultured HeLa S3 cells, in agreement with other recent studies (Grüneberg et al., 2006; Kamijo et al., 2006). This suggests that the relatively restricted phenotype seen in Citron kinase$^{-/-}$ mice reflect functional redundancy between structurally related kinases.

The tightly controlled localization of Ect2 suggested that a localized population of Ect2 might activate RhoA locally, thereby ensuring cleavage furrow formation at a position determined by the central spindle. Somewhat surprisingly, we found that endogenous Ect2 could be largely displaced from the central spindle without abolishing cytokinesis. Although it is difficult to exclude the fact that in cells overexpressing N-terminal Ect2 fragments, very low amounts of Ect2 might have persisted at the central spindle, these results indicate that physiological levels of Ect2 activity need not be present at this location for cytokinesis to occur. This conclusion is supported by other, more indirect studies (Mollinari et al., 2005; Yüce et al., 2005). Thus, the cortical pool of Ect2 is likely to be important for cytokinesis. How active RhoA is targeted to the cleavage furrow in cells harboring delocalized Ect2 is clearly an important question. One possibility is that landmarks are present at the site of cleavage furrow formation to direct proper RhoA-GTP localization. If so, this would indicate that other microtubule-dependent factors contribute to specify the site of cleavage furrow formation.

Displacement of Ect2 from the central spindle causes membrane blebbing

One remarkable consequence of displacing Ect2 from the central spindle was extensive membrane blebbing. Such blebbing is suggestive of highly dynamic cortical cytoskeletal rearrangements, probably brought about by RhoA-mediated remodelling of the cortical actomyosin system (Charras et al., 2005). In support of this view, overexpression of constitutively active RhoA, or dominant-negative MgcRacGAP, induces membrane blebbing (Lee et al., 2004), whereas depletion of RhoA suppresses membrane blebbing (Niiya et al., 2005). Thus, the blebbing seen in cells with displaced endogenous Ect2 could be caused by mislocalized RhoA-GTP, indicating that the association of Ect2 with the central spindle is crucial for restricting the localization of active RhoA-GTP.

Interference with abscission by persistence of midbody-associated Ect2 fragments

Overexpression of an N-terminal Ect2$_{1\text{-}333}$ caused extensive abscission failure, whereas a slightly longer fragment (Ect2$_{1\text{-}420}$) had no significant effect. To explain the dramatic phenotype produced by the Ect2$_{1\text{-}333}$ fragment, two explanations have previously been proposed. First, the cytokinesis failure was interpreted to reflect the inhibition of endogenous Ect2 activity, leading to low RhoA-GTP levels (Kimura et al., 2000). Although this view is supported by data indicating that the N- and C-termini of Ect2 are able to interact (Saito et al., 2004), our present data show that RhoA still localized to the cleavage furrow in cells harboring Ect2$_{1\text{-}333}$, and, as reported recently, this pool of RhoA represents the GTP-bound form (Yüce et al., 2005). Moreover, the extensive membrane blebbing seen in these cells further argues for the presence of active RhoA-GTP at the cortex. Most importantly, our data show that Ect1$_{1\text{-}333}$ does not prevent cleavage furrow ingression but subsequent abscission.

Another previous interpretation of the cytokinesis failure produced by the Ect2$_{1\text{-}333}$ fragment was based on the cytoplasmic localization of this fragment. Specifically, it has been argued that Ect2$_{1\text{-}333}$ could prematurely occupy binding sites for endogenous Ect2 (i.e. before nuclear envelope breakdown), thus acting as a dominant-negative mutant (Saito et al., 2003). However, we show here that endogenous Ect2 could also be displaced from the central spindle by Ect2 fragments that were unable to interfere with cytokinesis, suggesting that competition for Ect2 binding sites may not be the key for understanding the phenotype produced by Ect2$_{1\text{-}333}$. Instead, our data lead us to propose an alternative

interpretation. Specifically, we conclude that although the nucleo-cytoplasmic distribution of different Ect2 mutants may contribute to determine their ability to interfere with abscission, this is not the main determinant. Although all N-terminal Ect2 fragments able to interfere with cytokinesis also localized to the cytoplasm, and although the addition of a functional NLS to one such fragment partially restored abscission, we emphasize that not all N-terminal fragments showing a defect in nuclear import interfered with cytokinesis. This indicates that although re-import of these Ect2 fragments into the reforming telophase nucleus contributes to the successful completion of abscission, cytoplasmic localization per se does not produce abscission failure. Instead, we discovered that all inhibitory N-terminal fragments of Ect2 localized to a ring-like structure in the vicinity of the midbody. Similarly, *Drosophila pbl* was also shown to localize predominantly to a cortical ring-like structure, where it interacts with RacGAPc50 (Somers and Saint, 2003). We therefore propose that it is the sustained presence of Ect2$_{1-333}$ in these ring-like structures that causes the observed abscission failure. Based on these data, we consider it attractive to suggest that, under normal conditions, endogenous midbody-localized Ect2 could have a function in preventing pre-mature cell abscission, thereby contributing to the coordination of proper chromosome segregation with abscission.

In conclusion, our study strengthens the view that Ect2 is a key component of the molecular machinery that brings about cytokinesis. We have identified both interaction partners and regulatory domains within Ect2 and demonstrate that the precise temporal and spatial regulation of this GEF is crucial for cleavage furrow formation and ingression as well as abscission. Continued studies of the regulation and function of Ect2 will undoubtedly contribute to a better understanding of the regulatory circuits that control cytokinesis.

Materials and Methods

Plasmid constructions and site directed mutagenesis

Full-length human *ECT2* cDNA was amplified from a HeLa S3 cDNA library (Clontech Laboratories) using pfu DNA polymerase and cloned into a pCDNA3.1/3×myc vector in-frame with sequences that encode three N-terminal myc tags. Deletion constructs and point mutations were created by PCR using specific oligonucleotides and pfu DNA polymerase. All constructs were confirmed by DNA sequencing (Medigenomix). The plasmid containing the hWW45 cDNA has been described before (Chan et al., 2005).

Antibodies

Polyclonal rabbit human Ect2 antibodies were generated against an N-terminal His$_6$-tagged Ect2 fragment (residues 1-388) (Elevage Scientifique des Dombes, Chatillon sur Chalarone). Antibodies were affinity-purified, using the Ect2 antigen immobilized on nitrocellulose membrane (Schleicher & Schuell). A rabbit polyclonal antibody against human MgcRacGAP was raised using a C-terminal peptide (CSKSKSATNLGRQGN) coupled to keyhole limpet hemocyanin (Sigma Genosys) and antibodies were affinity-purified essentially as described (Kufer et al., 2002). Affinity-purified rabbit polyclonal human MKlp1 and MKlp2 sera were gifts from Thomas Mayer (Max-Planck-Institute for Biochemistry, Martinsried, Germany).

siRNA experiments

For siRNA, the following target sequences were used: Ect2, 5′-AAG AGU GGU UCU GGG GAA GCA-3′, 5′-AAA UAC UGC UGU GAA UCU AUU-3′ and 5′-CAU UUG AUA UGA AGC GUU AUU-3′; MgcRacGAP, 5′-AAG UGG CAG AGG ACU GAC CAU-3′; MKlp1, 5′-AAG CAG UCU UCC AGG UCA UCU-3′; MKlp2, 5′-AAC CAC CUA UGU AAU CUC AUG-3′; Aurora-B, 5′-AAG GUG AUG GAG AAU AGC AGU-3′. Oligonucleotides were annealed and transfected with oligofectamine (Life Technologies) as described (Elbashir et al., 2001). As a control, the GL-2 duplex, targeting the luciferase gene was used (Elbashir et al., 2001).

Cell culture and generation of inducible stable cell lines

HeLa S3 cells were grown at 37°C under 5% CO_2 in DMEM, supplemented with 10% FCS and penicillin-streptomycin (100 IU/ml and 100 μg/ml, respectively). For the generation of tetracycline-inducible cell lines the plasmid encoding myc-tagged Ect2$_{1-333}$ was transfected into a HeLa S3 cell line, which stably expressed a CMV-controlled tet repressor together with a blasticidine-resistance marker (pcDNA6/TR, Invitrogen). Stably transfected cell lines were established by selection with 5 μg/ml blasticidin and 1 μg/ml puromycin. The expression of myc-Ect2$_{1-333}$ was induced by addition of 1 μg/ml tetracycline for 24 hours. Transient transfections of HeLa S3 cells were performed using the Fugene6 (Roche) transfection method according to manufacturer's instructions.

Cell extracts, immunoprecipitations and western blot analysis

To enrich cells in anaphase and telophase of the cell cycle, HeLa S3 cells were first treated with 1.6 μg/ml aphidicolin for 17 hours, released for 6 hours into fresh growth medium, and then treated for 8 hours with 50 ng/ml nocodazole. Mitotic cells were collected by shaking off and then released for about 100 minutes into fresh medium during which time mitotic progression was monitored by fluorescence microscopic analysis of DAPI-stained cell samples. Cell extracts were prepared as described (Hanisch et al., 2006). Protein concentrations were determined using the Dc protein assay (Bio-Rad). For immunoprecipitations, 10 μg of polyclonal antibodies coupled to Affi-prep proteinA support (Bio-Rad) were used, except for myc-tagged recombinant proteins, which were isolated using anti-myc 9E10 monoclonal antibodies bound to Immunopure immobilized protein G (Pierce) resin. For western blotting, equal amounts of protein were separated by SDS-PAGE, followed by transfer to nitrocellulose membranes (Schleicher & Schuell). Membranes were probed with the following antibodies in PBS containing 0.05% Tween-20 and 5% non-fat milk: affinity-purified rabbit anti-Ect2 (1 μg/ml), chicken anti-MgcRacGAP (R&D systems, 1 μg/ml), affinity-purified rabbit MKlp1 (0.5 μg/ml), rabbit MKlp2 serum (1:1000), monoclonal anti-myc 9E10 (1:10 culture supernatant), monoclonal anti-α-tubulin (Sigma-Aldrich, 1:3000). Signals were detected by ECL SuperSignal (Pierce).

Immunofluorescence microscopy

Cells were grown on coverslips and fixed with 3% paraformaldehyde in 2% sucrose for 10 minutes or with 10% TCA for 15 minutes (only for visualizing RhoA). Cells were subsequently permeabilized with ice-cold 0.5% Triton X-100 for 5 minutes. Alternatively, cells were simultaneously fixed and permeabilized in PTEMF (20 mM PIPES pH 6.8, 4% formaldehyde, 0.2% Triton X-100, 10 mM EGTA, 1 mM $MgCl_2$) for 10 minutes at room temperature (RT). Cells were blocked for 30 minutes at RT in blocking solution (PBS, 1% BSA) and incubated for 1 hour with the following primary antibodies: purified rabbit anti-Ect2 (1 μg/ml), rabbit anti-C-terminal Ect2 (Santa Cruz Biotechnology, 1:200), rabbit purified anti-MgcRacGAP (1 μg/ml), rabbit anti-MKlp1 (Santa Cruz Biotechnology, 1:200), AIM-1 monoclonal against human Aurora-B (Becton Dickinson, 1:200), mouse monoclonal anti-RhoA (Santa Cruz Biotechnology, 1:200), mouse monoclonal anti-Citron kinase (BD Transduction laboratories 1:200), rabbit polyclonal anti-MKlp2 serum (1:2000). Primary antibodies were detected with Alexa Fluor 488- and Alexa Fluor 555-conjugated goat anti-mouse or anti-rabbit IgGs (1:1000, Molecular Probes), respectively. DNA was stained with 4′,6-diamidino-2-phenylindole (DAPI, 2 μg/ml). Immunofluorescence microscopy was performed using a Zeiss Axioplan II microscope with Apochromat 40× and 63× oil-immersion objectives, respectively, as described (Hanisch et al., 2006). For high-resolution images, a Deltavision microscope on an Olympus IX71base (Applied Precision, Issaquah, WA), equipped with PlanApo 60×/1.40 and UplanApo 100×/1.35 oil-immersion objectives (Olympus) and a CoolSNAP HQ camera (Photometrics) was used for collecting optical sections in the *z*-axis. Images at single focal planes were processed with a deconvolution algorithm, and optical sections were projected into one picture using Softworx software (Applied Precision). Images were cropped in Adobe Photoshop 6.0, and then sized and placed in figures using Adobe Illustrator 10 (Adobe Systems, San Jose, CA).

For live-cell imaging of the inducible myc-Ect2$_{1-333}$ stable cell line, cells were first treated with aphidicolin (1.6 μg/ml) for 16 hours to arrest them in G1-S. Cells were then released by three washes with PBS and tetracycline (1 μg/ml) in growth medium was added to induce myc-Ect2$_{1-333}$ expression. After 8 hours, the medium was changed to CO_2-independent medium (Invitrogen) supplemented with 10% calf serum and tetracycline. Live cell imaging was performed with a Zeiss Axiovert-2 microscope with a Plan Neofluar 40× objective, using a heated sample stage. Metaview software (Visitron Systems, Puchheim, Germany) was used to collect and process data. Images were captured with 10 millisecond exposure times at 2-minute intervals for 16 hours. For live-cell imaging of HeLa S3 cells treated with siRNAs, cells were transfected and simultaneously arrested at G1-S with aphidicolin. After 16 hours, cells were washed three times with PBS and released into fresh medium. About 8 hours after release, the medium was changed to CO_2-independent medium containing 10% calf serum and live-cell imaging was performed as described above.

We thank Francis Barr and Thomas Mayer (both MPI for Biochemistry) for antibodies and for helpful discussions. This work

was supported by the Max-Planck Society, the Deutsche Forschungsgemeinschaft (SFB 646), and the Fonds der Chemischen Industrie (to E.A.N.).

References

Barr, F. A., Sillje, H. H. and Nigg, E. A. (2004). Polo-like kinases and the orchestration of cell division. *Nat. Rev. Mol. Cell Biol.* **5**, 429-440.

Bement, W. M., Benink, H. A. and von Dassow, G. (2005). A microtubule-dependent zone of active RhoA during cleavage plane specification. *J. Cell Biol.* **170**, 91-101.

Blomberg, N., Baraldi, E., Nilges, M. and Saraste, M. (1999). The PH superfold: a structural scaffold for multiple functions. *Trends Biochem. Sci.* **24**, 441-445.

Chan, E. H., Nousiainen, M., Chalamalasetty, R. B., Schafer, A., Nigg, E. A. and Silljé, H. H. W. (2005). The Ste20-like kinase Mst2 activates the human large tumor suppressor kinase Lats1. *Oncogene* **24**, 2076-2086.

Charras, G. T., Yarrow, J. C., Horton, M. A., Mahadevan, L. and Mitchison, T. J. (2005). Non-equilibration of hydrostatic pressure in blebbing cells. *Nature* **435**, 365-369.

Clapperton, J. A., Manke, I. A., Lowery, D. M., Ho, T., Haire, L. F., Yaffe, M. B. and Smerdon, S. J. (2004). Structure and mechanism of BRCA1 BRCT domain recognition of phosphorylated BACH1 with implications for cancer. *Nat. Struct. Mol. Biol.* **11**, 512-518.

D'Avino, P. P., Savoian, M. S. and Glover, D. M. (2004). Mutations in sticky lead to defective organization of the contractile ring during cytokinesis and are enhanced by Rho and suppressed by Rac. *J. Cell Biol.* **166**, 61-71.

D'Avino, P. P., Savoian, M. S. and Glover, D. M. (2005). Cleavage furrow formation and ingression during animal cytokinesis: a microtubule legacy. *J. Cell Sci.* **118**, 1549-1558.

Devore, J. J., Conrad, G. W. and Rappaport, R. (1989). A model for astral stimulation of cytokinesis in animal cells. *J. Cell Biol.* **109**, 2225-2232.

Di Cunto, F., Imarisio, S., Hirsch, E., Broccoli, V., Bulfone, A., Migheli, A., Atzori, C., Turco, E., Triolo, R., Dotto, G. P. et al. (2000). Defective neurogenesis in citron kinase knockout mice by altered cytokinesis and massive apoptosis. *Neuron* **28**, 115-127.

Echard, A., Hickson, G. R., Foley, E. and O'Farrell, P. H. (2004). Terminal cytokinesis events uncovered after an RNAi screen. *Curr. Biol.* **14**, 1685-1693.

Eda, M., Yonemura, S., Kato, T., Watanabe, N., Ishizaki, T., Madaule, P. and Narumiya, S. (2001). Rho-dependent transfer of Citron-kinase to the cleavage furrow of dividing cells. *J. Cell Sci.* **114**, 3273-3284.

Elbashir, S. M., Harborth, J., Lendeckel, W., Yalcin, A., Weber, K. and Tuschl, T. (2001). Duplexes of 21-nucleotide RNAs mediate RNA interference in cultured mammalian cells. *Nature* **411**, 494-498.

Fujiwara, T., Bandi, M., Nitta, M., Ivanova, E. V., Bronson, R. T. and Pellman, D. (2005). Cytokinesis failure generating tetraploids promotes tumorigenesis in p53-null cells. *Nature* **437**, 1043-1047.

Glotzer, M. (2001). Animal cell cytokinesis. *Annu. Rev. Cell Dev. Biol.* **17**, 351-386.

Glotzer, M. (2005). The molecular requirements for cytokinesis. *Science* **307**, 1735-1739.

Gromley, A., Yeaman, C., Rosa, J., Redick, S., Chen, C. T., Mirabelle, S., Guha, M., Sillibourne, J. and Doxsey, S. J. (2005). Centriolin anchoring of exocyst and SNARE complexes at the midbody is required for secretory-vesicle-mediated abscission. *Cell* **123**, 75-87.

Gruneberg, U., Neef, R., Honda, R., Nigg, E. A. and Barr, F. A. (2004). Relocation of Aurora B from centromeres to the central spindle at the metaphase to anaphase transition requires MKlp2. *J. Cell Biol.* **166**, 167-172.

Grüneberg, U., Neef, R., Li, X., Chan, E. H. Y., Chalamalasetty, R. B., Nigg, E. A. and Barr, F. A. (2006). KIF14 and citron kinase act together to promote efficient cytokinesis. *J. Cell Biol.* **172**, 363-372.

Guse, A., Mishima, M. and Glotzer, M. (2005). Phosphorylation of ZEN-4/MKLP1 by aurora B regulates completion of cytokinesis. *Curr. Biol.* **15**, 778-786.

Hanisch, A., Wehner, A., Nigg, E. A. and Sillje, H. H. (2006). Different Plk1 functions show distinct dependencies on polo-box domain-mediated targeting. *Mol. Biol. Cell* **17**, 448-459.

Hill, E., Clarke, M. and Barr, F. A. (2000). The Rab6-binding kinesin, Rab6-KIFL, is required for cytokinesis. *EMBO J.* **19**, 5711-5719.

Hime, G. and Saint, R. (1992). Zygotic expression of the pebble locus is required for cytokinesis during the postblastoderm mitoses of Drosophila. *Development* **114**, 165-171.

Hirose, K., Kawashima, T., Iwamoto, I., Nosaka, T. and Kitamura, T. (2001). MgcRacGAP is involved in cytokinesis through associating with mitotic spindle and midbody. *J. Biol. Chem.* **276**, 5821-5828.

Kamijo, K., Ohara, N., Abe, M., Uchimura, T., Hosoya, H., Lee, J. S. and Miki, T. (2006). Dissecting the role of Rho-mediated signaling in contractile ring formation. *Mol. Biol. Cell* **17**, 43-55.

Kim, J. E., Billadeau, D. D. and Chen, J. (2005). The tandem BRCT domains of Ect2 are required for both negative and positive regulation of Ect2 in cytokinesis. *J. Biol. Chem.* **280**, 5733-5739.

Kimura, K., Tsuji, T., Takada, Y., Miki, T. and Narumiya, S. (2000). Accumulation of GTP-bound RhoA during cytokinesis and a critical role of ECT2 in this accumulation. *J. Biol. Chem.* **275**, 17233-17236.

Kufer, T. A., Silljé, H. H. W., Korner, R., Gruss, O. J., Meraldi, P. And Nigg, E. A. (2002). Human TPX2 is required for targeting Aurora-A kinase to the spindle. *J. Cell Biol.* **158**, 617-623.

Kuriyama, R., Gustus, C., Terada, Y., Uetake, Y. and Matuliene, J. (2002). CHO1, a mammalian kinesin-like protein, interacts with F-actin and is involved in the terminal phase of cytokinesis. *J. Cell Biol.* **156**, 783-790.

Lee, J. S., Kamijo, K., Ohara, N., Kitamura, T. and Miki, T. (2004). MgcRacGAP regulates cortical activity through RhoA during cytokinesis. *Exp. Cell Res.* **293**, 275-282.

Lehner, C. F. (1992). The pebble gene is required for cytokinesis in Drosophila. *J. Cell Sci.* **103**, 1021-1030.

Liu, X. F., Ishida, H., Raziuddin, R. and Miki, T. (2004). Nucleotide exchange factor ECT2 interacts with the polarity protein complex Par6/Par3/protein kinase Czeta (PKCzeta) and regulates PKCzeta activity. *Mol. Cell. Biol.* **24**, 6665-6675.

Mabuchi, I., Hamaguchi, Y., Fujimoto, H., Morii, N., Mishima, M. and Narumiya, S. (1993). A rho-like protein is involved in the organisation of the contractile ring in dividing sand dollar eggs. *Zygote* **1**, 325-331.

Madaule, P., Eda, M., Watanabe, N., Fujisawa, K., Matsuoka, T., Bito, H., Ishizaki, T. and Narumiya, S. (1998). Role of citron kinase as a target of the small GTPase Rho in cytokinesis. *Nature* **394**, 491-494.

Margolis, R. L. (2005). Tetraploidy and tumor development. *Cancer Cell* **8**, 353-354.

Matuliene, J. and Kuriyama, R. (2002). Kinesin-like protein CHO1 is required for the formation of midbody matrix and the completion of cytokinesis in mammalian cells. *Mol. Biol. Cell* **13**, 1832-1845.

Meraldi, P., Honda, R. and Nigg, E. A. (2002). Aurora-A overexpression reveals tetraploidization as a major route to centrosome amplification in p53–/– cells. *EMBO J.* **21**, 483-492.

Miki, T., Smith, C. L., Long, J. E., Eva, A. and Fleming, T. P. (1993). Oncogene ect2 is related to regulators of small GTP-binding proteins. *Nature* **362**, 462-465.

Minoshima, Y., Kawashima, T., Hirose, K., Tonozuka, Y., Kawajiri, A., Bao, Y. C., Deng, X., Tatsuka, M., Narumiya, S., May, W. S., Jr et al. (2003). Phosphorylation by aurora B converts MgcRacGAP to a RhoGAP during cytokinesis. *Dev. Cell* **4**, 549-560.

Mishima, M., Kaitna, S. and Glotzer, M. (2002). Central spindle assembly and cytokinesis require a kinesin-like protein/RhoGAP complex with microtubule bundling activity. *Dev. Cell* **2**, 41-54.

Mollinari, C., Kleman, J. P., Saoudi, Y., Jablonski, S. A., Perard, J., Yen, T. J. and Margolis, R. L. (2005). Ablation of PRC1 by small interfering RNA demonstrates that cytokinetic abscission requires a central spindle bundle in mammalian cells, whereas completion of furrowing does not. *Mol. Biol. Cell* **16**, 1043-1055.

Naim, V., Imarisio, S., Di Cunto, F., Gatti, M. and Bonaccorsi, S. (2004). Drosophila citron kinase is required for the final steps of cytokinesis. *Mol. Biol. Cell* **15**, 5053-5063.

Neef, R., Preisinger, C., Sutcliffe, J., Kopajtich, R., Nigg, E. A., Mayer, T. U. and Barr, F. A. (2003). Phosphorylation of mitotic kinesin-like protein 2 by polo-like kinase 1 is required for cytokinesis. *J. Cell Biol.* **162**, 863-875.

Neef, R., Klein, U. R., Kopajtich, R. and Barr, F. A. (2006). Cooperation between mitotic kinesins controls the late stages of cytokinesis. *Curr. Biol.* **16**, 301-307.

Niiya, F., Xie, X., Lee, K. S., Inoue, H. and Miki, T. (2005). Inhibition of Cdk1 induces cytokinesis without chromosome segregation in an ECT2 and MgcRacGAP-dependent manner. *J. Biol. Chem.* **280**, 36502-36509.

Nishimura, Y. and Yonemura, S. (2006). Centralspindlin regulates ECT2 and RhoA accumulation at the equatorial cortex during cytokinesis. *J. Cell Sci.* **119**, 104-114.

Prokopenko, S. N., Brumby, A., O'Keefe, L., Prior, L., He, Y., Saint, R. and Bellen, H. J. (1999). A putative exchange factor for Rho1 GTPase is required for initiation of cytokinesis in Drosophila. *Genes Dev.* **13**, 2301-2314.

Saito, S., Tatsumoto, T., Lorenzi, M. V., Chedid, M., Kapoor, V., Sakata, H., Rubin, J. and Miki, T. (2003). Rho exchange factor ECT2 is induced by growth factors and regulates cytokinesis through the N-terminal cell cycle regulator-related domains. *J. Cell Biochem.* **90**, 819-836.

Saito, S., Liu, X. F., Kamijo, K., Raziuddin, R., Tatsumoto, T., Okamoto, I., Chen, X., Lee, C. C., Lorenzi, M. V., Ohara, N. et al. (2004). Deregulation and mislocalization of the cytokinesis regulator ECT2 activate the Rho signaling pathways leading to malignant transformation. *J. Biol. Chem.* **279**, 7169-7179.

Shandala, T., Gregory, S. L., Dalton, H. E., Smallhorn, M. and Saint, R. (2004). Citron kinase is an essential effector of the Pbl-activated Rho signalling pathway in Drosophila melanogaster. *Development* **131**, 5053-5063.

Shi, Q. and King, R. W. (2005). Chromosome nondisjunction yields tetraploid rather than aneuploid cells in human cell lines. *Nature* **437**, 1038-1042.

Somers, W. G. and Saint, R. (2003). A RhoGEF and Rho family GTPase-activating protein complex links the contractile ring to cortical microtubules at the onset of cytokinesis. *Dev. Cell* **4**, 29-39.

Storchova, Z. and Pellman, D. (2004). From polyploidy to aneuploidy, genome instability and cancer. *Nat. Rev. Mol. Cell Biol.* **5**, 45-54.

Tatsumoto, T., Xie, X., Blumenthal, R., Okamoto, I. and Miki, T. (1999). Human ECT2 is an exchange factor for Rho GTPases, phosphorylated in G2/M phases, and involved in cytokinesis. *J. Cell Biol.* **147**, 921-928.

Terada, Y., Tatsuka, M., Suzuki, F., Yasuda, Y., Fujita, S. and Otsu, M. (1998). AIM-1: a mammalian midbody-associated protein required for cytokinesis. *EMBO J.* **17**, 667-676.

Williams, R. S., Lee, M. S., Hau, D. D. and Glover, J. N. (2004). Structural basis of phosphopeptide recognition by the BRCT domain of BRCA1. *Nat. Struct. Mol. Biol.* **11**, 519-525.

Yüce, O., Piekny, A. and Glotzer, M. (2005). An ECT2-centralspindlin complex regulates the localization and function of RhoA. *J. Cell Biol.* **170**, 571-582.